Mon. Not. R. Astron. Soc. **324**, 33–50 (2001)

Magellanic Cloud WC/WO Wolf–Rayet stars – II. Colliding winds in binaries

P. Bartzakos,[1]★ A. F. J. Moffat[1]†‡ and V. S. Niemela[2]‡§

[1]*Département de physique, Université de Montréal, and Observatoire du Mont-Mégantic, PO Box 6128, Station Centre-Ville, Montréal, Québec, H3C 3J7, Canada*

[2]*Facultad de Ciencias Astronómicas y Geofísicas, Universidad Nacional de La Plata, Paseo del Bosque, 1900 La Plata, Argentina*

Accepted 2000 October 2. Received 2000 September 18; in original form 1999 July 28

ABSTRACT

A search for evidence of colliding winds is undertaken among the four certain Magellanic Cloud WC/WO spectroscopic binaries found in the companion Paper I, as well as among two Galactic WC/WO binaries of very similar subtype. Two methods of analysis, which allow the determination of orbital inclination and parameters relating to the shock cone from spectroscopic studies of colliding winds, are attempted. In the first method, Lührs' spectroscopic model is fitted to the moderately strong C III 5696-Å excess line emission arising in the shock cone for the stars Br22 and WR 9. The four other systems show only very weak C III 5696-Å emission. Lührs' model follows well the mean displacement of the line in velocity space, but is unable to reproduce details in the line profile and fails to give a reliable estimate of the orbital inclination. In the second method, an alternative attempt is also made to fit the variation of more global quantities, full width at half-maximum and radial velocity of the excess emission, with phase. This method also gives satisfactory results in a qualitative way, but shows numerical degeneracy with orbital inclination. Colliding wind effects on the very strong C IV 5808-Å Wolf–Rayet emission line, present in all six binaries, are also found to behave qualitatively as expected. After allowing for line enhancement in colliding wind binaries, it now appears that *all* Magellanic Cloud WC/WO stars occupy a very narrow range in spectral subclass: WC4/WO3.

Key words: shock waves – binaries: spectroscopic – stars: Wolf–Rayet – Magellanic Clouds.

1 INTRODUCTION

The winds of main-sequence massive stars have similar terminal wind velocities ($\langle v_\infty \rangle \approx 2000\,\mathrm{km\,s^{-1}}$) to those of their descendent Wolf–Rayet (WR) stellar winds. However, with $\langle \dot{M} \rangle \approx 10^{-5}\,\mathrm{M_\odot\,yr^{-1}}$, WR winds tend to be at least an order of magnitude denser than those of main-sequence OB stars (e.g. Maeder & Conti 1994). With these values, the mechanical energy $\frac{1}{2}\dot{M}v_\infty^2$ can range up to several per cent of the total output of the star.

In a massive, hot binary system, both winds can be expected to collide with one another and form a shock zone, with the release of a good fraction of the mechanical and thermal energy in various forms. If both winds are of equal momentum flux, a planar shock zone will be formed mid-way between and perpendicular to the axis joining the two stars. In the case of WR+O binaries, the stronger wind of the WR star will create a bow shock, the concave side of which will curve towards the companion O star in the form of a shock cone (e.g. Stevens, Blondin & Pollock 1992). Formally, if one wind is significantly stronger than that of its companion, the wind could strike the photosphere of the companion. However, sudden radiative braking, the reflection and absorption of O-star photons on the metal-rich WR wind material just before collision, could weaken its effective momentum flux sufficiently to prevent the wind of the primary from striking the O star and render the shock cone more planar (e.g. Gayley, Owocki & Cranmer 1997).

Various workers have predicted or observed effects that are attributed to colliding winds between hot stars. Of particular note are the X-ray fluxes. Prilutskii & Usov (1976), as well as Cherepaschuk (1976), predicted shock temperatures of the order of 10^6 K, which should produce X-ray fluxes in WR+O systems that are much higher than those for single WR or O stars. However, such high X-ray fluxes have not been found in general (Corcoran et al. 1996); perhaps radiative braking, combined with

★ E-mail: bartzako@astro.umontreal.ca

† Killam Fellow of the Canada Council for the Arts.

‡ Visiting Astronomer, Cerro Tololo Interamerican Observatory, National Optical Astronomy Observatories.

§ Member of Carrera del Investigador, CIC, Prov. Buenos Aires, Argentina.

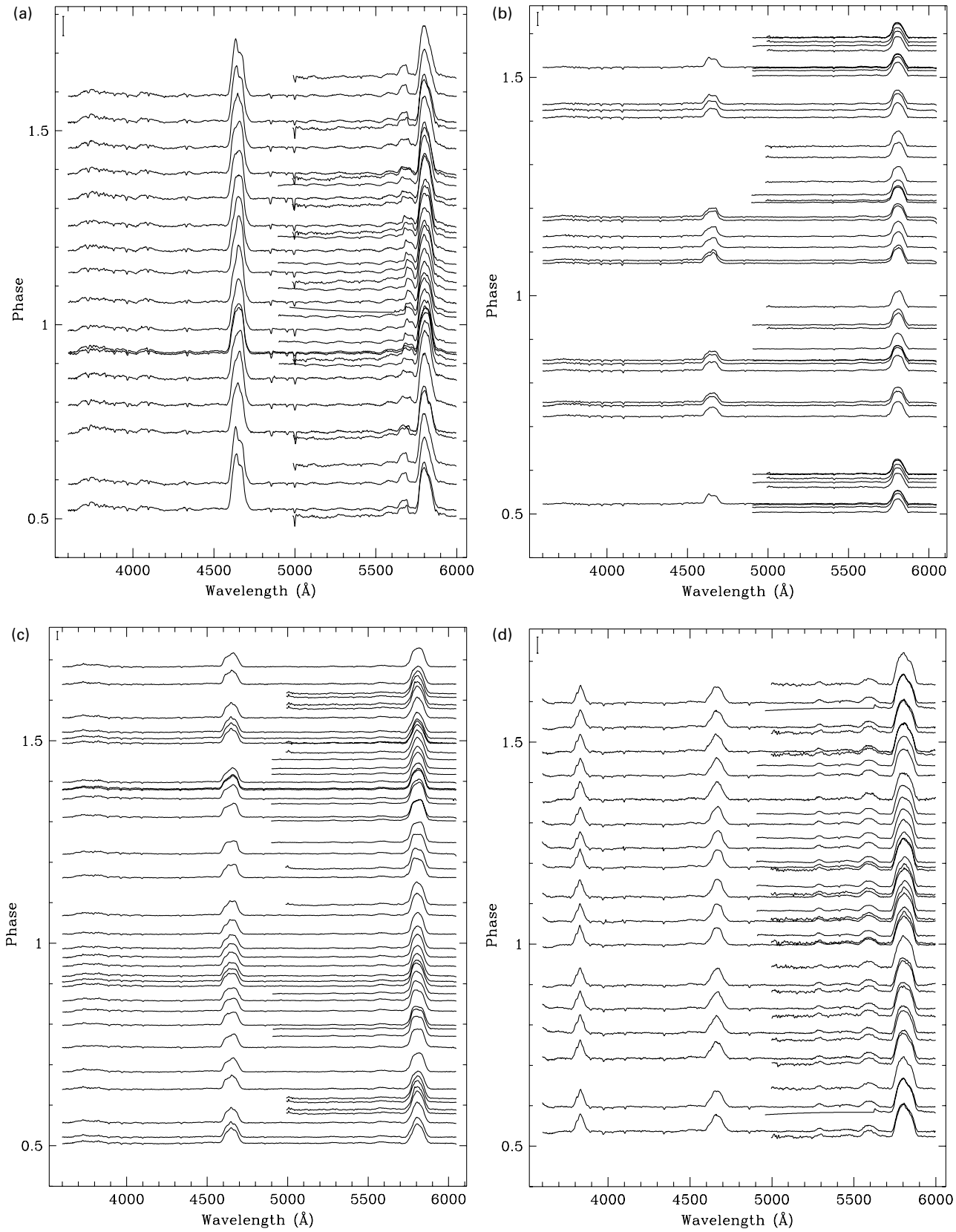

Figure 1. (a) Montage of phased Br22 spectra. The bar in the upper left-hand corner shows the intensity of the continuum. (b) As (a), but for Br31. (c) As (a), but for Br32. (d) As (a), but for AB8. (e) As (a), but for WR 9. (f) As (a), but for WR 30a.

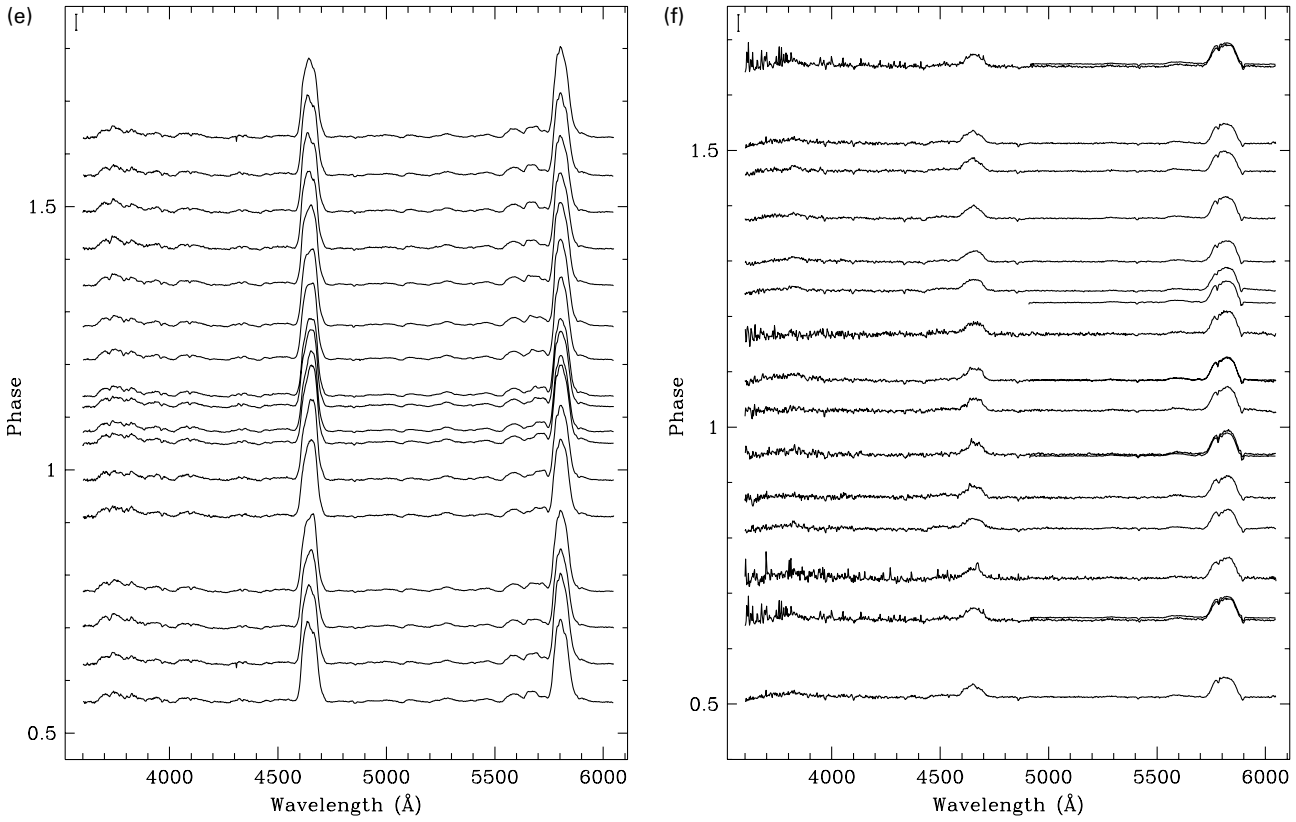

Figure 1 – *continued*

wind clumping, dampens the force of the collision, hindering attainment of the expected high temperature and X-ray fluxes.

The geometric distortion, introduced in the orbital system by colliding winds, could translate into perturbed spectroscopic lines, either by some form of occultation or displacement of the stellar wind or by excess emission from cooling material that is initially heated to very high temperature by the winds striking each other near the bow head. Possibly, these effects could be measured and their variation with orbital phase be examined, in order to determine various parameters related to the two winds, their collision process and the geometry of the orbit itself. One conceivable parameter is the orbital inclination. If so, this could render spectroscopy a very useful tool to provide an orbital constraint that could only be obtained previously with more difficult techniques, such as polarimetry or photometry. In this way, spectroscopy alone would allow a convenient, reliable and complete determination of masses in binary stars.

This second of a pair of papers on the WC/WO class of WR stars of the Magellanic Clouds reports time-resolved optical spectroscopy of wind–wind collisions (WWCs) for those stars found to be definitely binary: Br22, Br31, Br32 and AB8 (Bartzakos, Moffat & Niemela 2001, hereafter Paper I). The Galactic stars WR 9 and WR 30a, of similar spectral subclass, are also included for comparison. The emphasis is on the obvious variation of the C III 5696-Å line of Br22 (and WR 9), with the results of an attempt to fit a Lührs model to the profiles, assuming that their variation is due to colliding winds. A study of FWHM and mean radial velocity variations of the excess emission profiles is also made in an attempt to model the wind and determine parameters such as flow speed, cone opening angle and orbital inclination. Qualitative study of the much more subtle variation of the strong C IV 5808-Å line is also included. All six WR+O binaries contain hot WC/WO stars of subtype WC4 (Br22, Br31, Br32, WR 9), WO3 (AB8) or WO4 (WR 30a), after allowing for the impact of the excess emission itself on the spectral classifications.

2 OBSERVATIONS AND DATA REDUCTION

Spectroscopic data on the four binary WC/WO Magellanic Cloud stars, as well as on the two Galactic WC stars, cited at the end of Section 1, were collected during three observing runs, in 1984 December, 1993 January and 1993 November. All three runs were undertaken using charge-coupled device detectors and diffraction grating spectrometers. The technical specifications and procedures are as outlined in Paper I and in Bartzakos (1998). The latter also includes more detailed descriptions.

3 COLLIDING WINDS AND SHOCK CONE PARAMETERS

3.1 The spectra

Montages of phase-sorted spectra of the six studied binaries are illustrated in Fig. 1 (mean spectra are given in Paper I). The phases were determined from the orbits deduced using the same data (described in Appendix A).

Among the four Magellanic Cloud WC/WO+O binaries (in fact among all 24 Magellanic Cloud WC/WO stars discussed in Paper I), Br22 is special because it is the only Magellanic Cloud WC/WO star to exhibit moderately strong C III 5696-Å emission. This line is also highly variable. In addition, it shifts in a very high-amplitude sinusoidal pattern with the orbital period, but

approximately one-quarter of an orbit behind the WR orbit. The emission must probably come from a part of the binary system other than the WR star.

Another interesting feature of the C III 5696-Å line in Br22 is that it varies in form as well as in position. It is wider at some phases and its asymmetry changes: the blue wing is sometimes more intense than the red wing and vice versa at other times. As shown in the next subsections, this is the behaviour expected if the variable C III emission arises in a shock cone that wraps around the weaker-wind O star, with a flow pattern directed away from the WR star.

The same phenomenon is seen in WR 9 (Fig. 1). However, there appears to be a non-negligible base C III 5696-Å emission in WR 9 upon which excess emission moves independently of the base. Apparently, the inherent C III line emission from the WR star is stronger here than in Br22, although, in an absolute sense, it is still relatively weak.

Besides the C III 5696-Å line, other lines (mostly the stronger lines) in Br22 and the five other binaries do vary. However, these variations are more subtle, since they are superposed on much brighter emission lines produced in the WR wind. Do these variations also arise in the WWC zone? An attempt to answer this will be described later in Section 3.4, after dealing with an emission-excess model for the WWCs.

Why is C III 5696-Å excess only seen in Br22 and WR 9 among the six WC+O binaries, even though these WC/WO subtypes are all very similar? Usov (private communication) has studied the energy produced in WWCs; it tends to peak in WR+O systems of intermediate orbital separation (or periods of the order of a month), as is the case for Br22 and WR 9. Radiative braking might also play a role, especially in close systems and when the WR wind strongly exceeds the O-star wind, by preventing the WR wind from reaching its full speed and reducing the force of the WWC, changing the conditions in which the ions are created. Not all ions that could be theoretically expected in a collision without radiative braking might form in such a case, and those that do might not be as abundant (perhaps the C III excess even in Br22 and WR 9 might have been greater without radiative braking). However, AB8 has a similar period compared to Br22 and WR 9; presumably its WWC zone does not lead to C III excess for a different reason: its WO component has a much hotter, O-richer wind.

Why is C III 5696 Å enhanced more than other lines in Br22 and WR 9? Empirically, this line appears to be very sensitive to wind clumping in single WC stars (e.g. Moffat 1996), and so also sensitive to density enhancements as expected in WWC zones. Theoretically, C III 5696 Å is more sensitive to density enhancements than other lines (Hillier, private communication).

3.2 Modeling C III 5696 Å with the Lührs profile

Lührs (1991, 1997) developed an analytical function for the line profile from WWC excess emission originating from a band around the shock cone. In this geometrical model, for a given line emission, he took into account the cone opening half-angle, θ, and its thickness, the streaming velocity of the material along the cone, $v_{\rm strm}$, the inclination of the orbital plane to the observer, i, and the phase of observation, φ, adjusted for the shift in the axis of the cone angle, $\delta\varphi$, owing to the Coriolis forces associated with the orbital motion (see Fig. 2). Lührs also made the reasonable assumption that the angular dependence of the matter density in the streaming region of the shock cone can be described by a parabolic function of $\cos\theta$. This function is equal to zero at the boundaries (θ_1 and θ_2) and is a maximum halfway between in $\cos\theta$. Examples of Lührs' model as a function of phase for various orbital inclinations and cone opening half-angles are shown graphically in Fig. 3. Note that the effects of the different parameters of the model are coupled. The weakness of the Lührs model is the lack of hydrodynamic and radiation physics. However, this is also its strength: simplicity.

Lührs fitted this model to the C III 5696-Å excess emission line of individual spectra for the 9 d period WC7+O5–7 binary WR 79 to derive a global set of mean parameters. An attempt is made, here, to find the parameters by fitting the profile curves to all the excess emission-line data for Br22 *simultaneously* [cf. Hill et al. (2000) for WR 42 – another (8 d) WC7+O7 binary – and WR 79].

Before a fit was carried out, an estimate of the base profile of C III 5696 Å inherent in the wind of the WR star was made. All of the 1993 November spectra of the star were shifted to the frame of reference of the WR star by subtracting the orbital velocity measured from the C IV 5808-Å emission line of each spectrum. All spectra were then adjusted to the same wavelength dispersion and superimposed upon one another, and a minimum profile was defined by the lowest intensity of all spectra at each pixel (see Fig. 4).

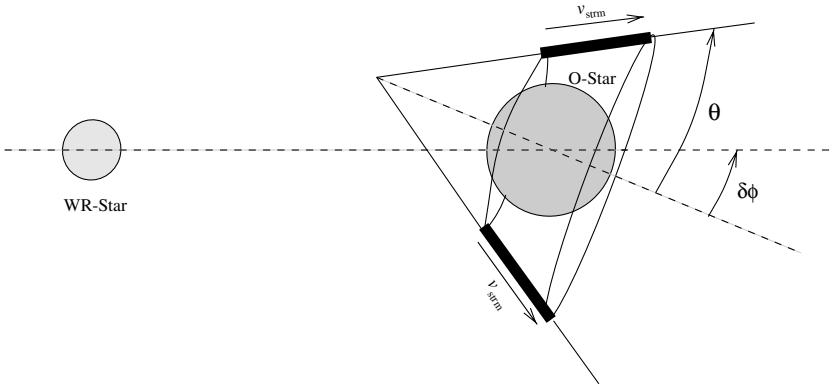

Figure 2. Lührs' model for an idealized optically thin region of emission where the shock cone has an opening half-angle θ and forms an angle $\delta\varphi$ with the line joining the two stars. Note that the dark rectangles represent only a cross-section of the homogeneous region of emission (with streaming velocity $v_{\rm strm}$) around the three-dimensional conical surface.

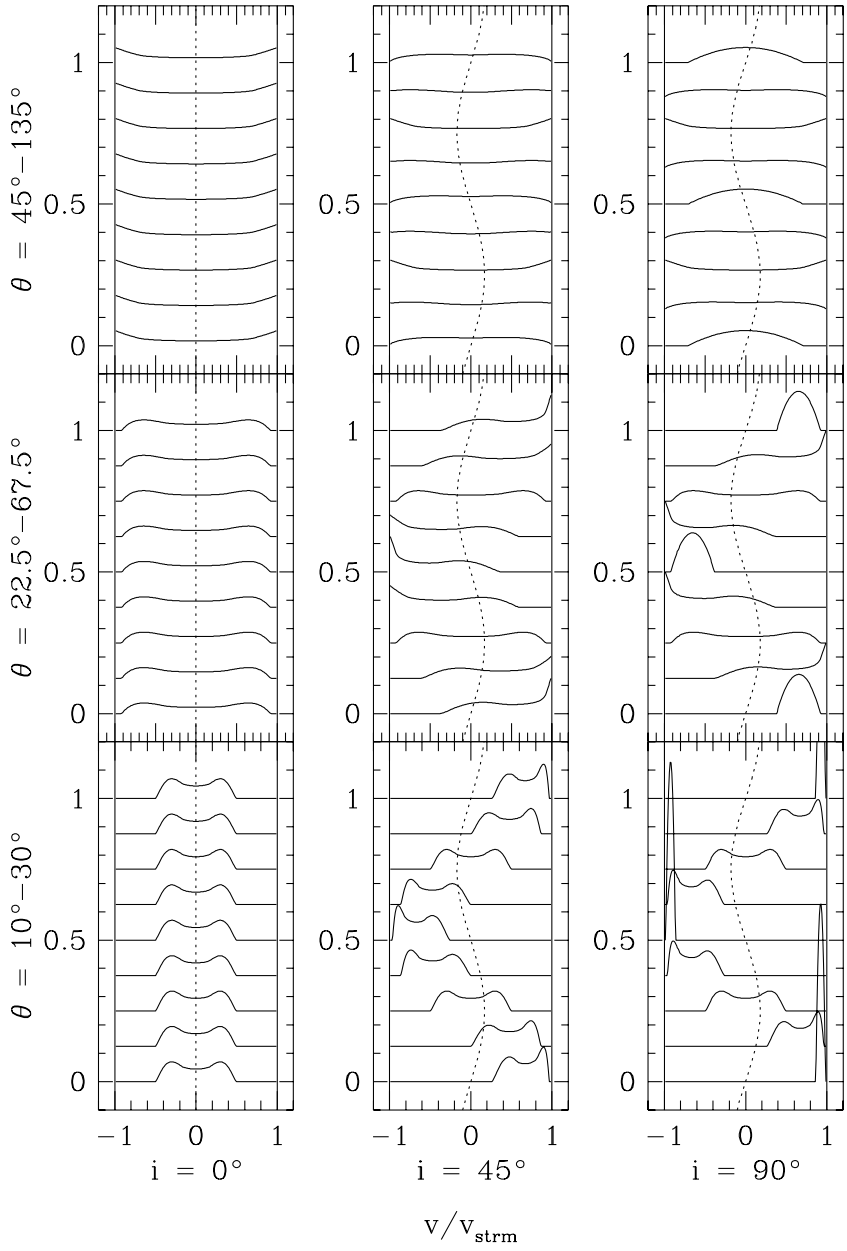

Figure 3. Examples of Lührs' profiles at various inclinations and phases with $\delta\varphi = 0$. The velocity scale is normalized to $v_{\rm strm}$. The dashed curve depicts the radial velocity orbit of the WR star (amplitude of $0.2v_{\rm strm}\sin i$). The range in cone opening half-angle θ goes from θ_1 to θ_2 in the context of the model such that $\Delta\theta \equiv \theta_2 - \theta_1 \approx \bar{\theta} \equiv (\theta_1 + \theta_2)/2$, i.e. the adiabatic case. Phase is shown on the ordinate of each plot where phase $\varphi = 0$ is when the WR star is in front of the O star. No instrumental smoothing has been carried out as would be necessary when fitting to real data.

The purpose of this minimum profile was to estimate the emission of C III 5696 Å inherent to the WR star (as opposed to that produced by excess emission in the WWC). This emission line is expected to be flat-topped. The peak in the minimum profile was, therefore, replaced by a line manually interpolated between the two wings of the minimum profile to yield, finally, the pedestal profile assumed for the WR star (dashed lines in Fig. 4).

This pedestal line was then subtracted from each spectrum (still in the WR frame) to estimate the net excess emission of C III arising from WWCs. [Subtracting the same flat profile at all phases is an approximation, since it is possible that different sections of the profile are partially deleted by the effect of the cavity created by the O-star wind, rendering the profile variable rather than constant. However, Hill et al. (2000) show that this effect is negligible in WR 42 and WR 79.] The orbital velocity shifts were then added back to return the excess emission profiles to the frame of the observer. These profiles are shown simultaneously with the fits below.

A non-linear, least-squares routine was used to fit the Lührs model to the excess emission-line data from the WWC. The fit parameters were θ_1, θ_2, i, $\delta\varphi$ and $v_{\rm strm}$. A zero-point velocity for the profiles, v_0, was included as a fit parameter, to locate the a priori unknown line centre of the normalized velocity $u = (v_{\rm obs} - v_0)/v_{\rm strm}$, where $v_{\rm obs}$ is the observed velocity of an element in the profile. A final parameter was a constant of proportionality for the intensity of the line, $I(u)$. Included in the fit was the convolution of the estimate of the instrumental profile

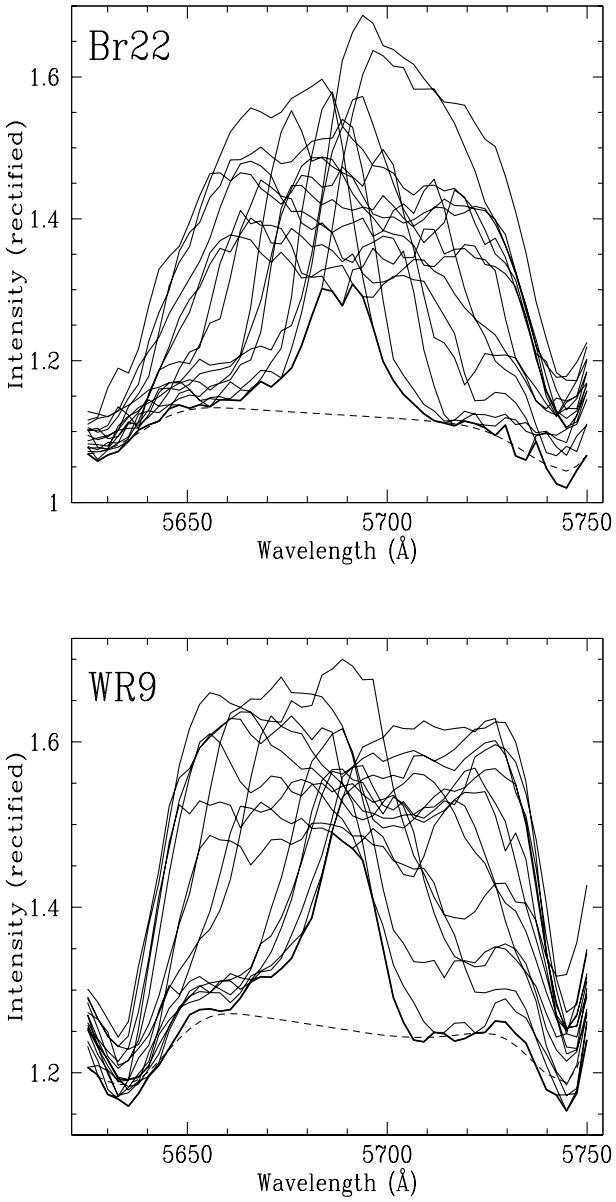

Figure 4. Superposition of spectra, minimum profile (thick line) and assumed pedestal WR-star emission of C III 5696 Å(dashed line) for Br22 and WR 9.

with the Lührs model. By examination of various emission lines of the comparison spectra taken along with the stellar spectra, this profile was determined to be well simulated by a Gaussian function of FWHM = 8.1 Å.

The χ^2 function of the calculated model as compared with the data was fitted with the routine PIKAIA [pre-release version (Charbonneau 1995)]. This was chosen since it is very effective for models that are highly non-linear, is very unlikely to find erroneously a solution that is at a secondary extremum, and requires no initial estimate of the solution.

A fit of the Lührs model, according to the above technique, was made simultaneously to the series of C III 5696-Åexcess line spectra in the best epoch of data, that of 1993 November for Br22. (The remaining epochs show similar variations, although with increased noise.) The results are shown in Fig. 5. It is apparent from the figure that the model qualitatively follows, with phase, the overall displacement and width of the profile very well. There are, however, discrepancies at the extremes of the line profiles. When the profile approaches its extreme red or blue displacement, the outer peak predicted by the theory does not appear clearly in the data. The values of the parameters of the best fit are listed in Table 1. The long process of calculating errors of the coefficients was not undertaken, given the systematic problems encountered. In any case, the inclination determined by the fit of the Lührs model is much smaller than that found by four other methods! A similar effect is found for a fit to the data of WR 9 (Fig. 6 and Table 2). However, application of the same fitting routine to the WR 42 and WR 79 data of Hill et al. (2000) yields good results.

What process can produce a spectroscopic profile where the peak at a velocity extremum is not produced? The first idea that comes to mind is some sort of occultation of the shock cone by the O star, so that the material that would produce the extreme peak is hidden from view. At any orbital phase, however, only the more redshifted material can be occulted by the O star. Only the reddened peak could be eliminated, yet the blue peak, when the profile is at its extreme blue velocity, is missing as well (cf. Fig. 5). Therefore occultation effects seem unlikely.

Another possibility might be that part of the underlying line profile of the WR star is deleted by the O-star wind and replaced by WWC emission at only slightly lower radial velocity seen by the observer (cf. Stevens & Howarth 1999). When the WR star is in front, the O-wind cavity occurs at high radial velocity in the C III base, thus depressing the outside (red) peak of the excess emission, as observed. When the WR star is behind, the blue peak is depressed, also as observed. At opposition, the cavity occurs close to zero radial velocity. However, Stevens & Howarth (1999) only had qualitative success with this hypothesis. In any case, the underlying WR C III 5696-Åline is extremely weak in Br22 and WR 9, so that this effect should not be a problem in these stars.

Yet another explanation that qualitatively works is as follows: when the shock cone is seen pointing away from the observer (maximum mean redshift) it is possible, in some systems, that its far edge is observed along the line of sight (i.e. $\bar{\theta} \approx i$). Under these conditions the emission from this part of the cone, moving at approximately constant speed at different distances along the cone, could be optically thick and so reduced in intensity. This corresponds to the red peak. When the shock cone points towards the observer (maximum mean blueshift), the same reasoning explains the reduction of the blue peak intensity. However, this explanation requires special conditions and is therefore less appealing.

A fourth possibility, as noted by Stevens & Howarth (1999), is enhancement of the emission from the trailing edge of the shock cone. This tends to strengthen the appropriate peak, as observed. Introducing this into the model is, however, beyond the scope of this investigation.

In any case, the true origin of this problem remains to be found with certainty. It could entail several or none of the above effects. It does not seem to be important in the Galactic WC7+O 8–9 d period binaries WR 42 and WR 79 (Hill et al. 2000), for reasons that are currently unclear. Perhaps the different WC subtypes and orbital periods play a role.

The deviating trends are even worse when Lührs' profile fits are made with fixed i (from polarimetry) as in Figs 5 and 6 (cf. Tables 1 and 2). This indeed suggests that the Lührs model requires significant modification, at least in the cases of Br22 and WR 9.

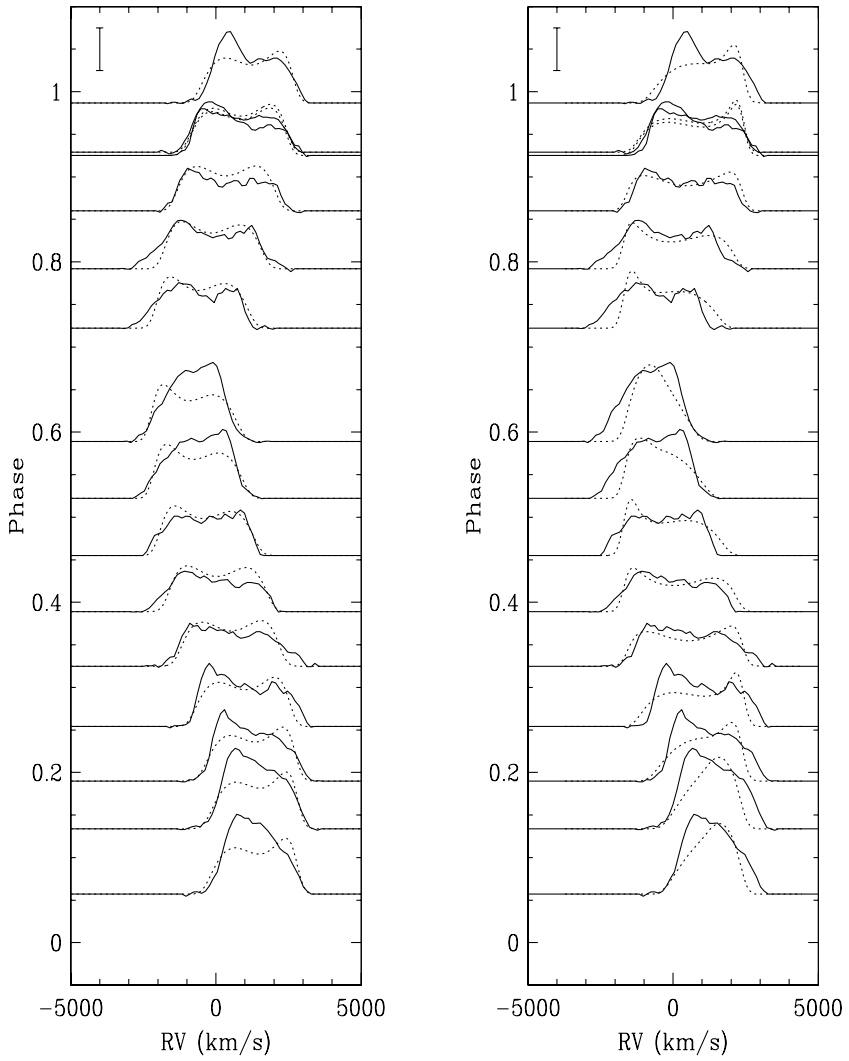

Figure 5. Lührs' model fit to the 1993 November C III 5696-Å spectra of Br22. The left-hand plot shows the fit for inclination as a variable parameter, while the right-hand side shows the results with a fixed inclination of $i = 71°$. The solid lines represent the data truncated to zero outside the excess profile, while the dotted lines show the corresponding instrumentally smoothed model fits. Here the wavelength is in the inertial frame of the centre of mass of the system. The vertical bar height indicates 25 per cent of the continuum intensity.

Table 1. Parameter values of the Lührs model fit to the 1993 November spectra of the CIII 5696-Å line for Br22 (for inclination both as a variable fit and as a fixed parameter). Included are results from an attempt to determine cone parameters from arbitrarily estimated peak locations (see Section 3.3) and the estimated inclination from other methods.

Parameter	Simultaneous fit	Simultaneous fit (fixed i)	Peak estimates[a]	Photometry[b]	Polarimetry[c]	Spectroscopy (O-star)[d]
θ_1 (degrees)	0.4	9	$\bar{\theta} = 47$	–	–	–
θ_2 (degrees)	45	90		–	–	–
i (degrees)	30	(71)	63	76	71	71
$\delta\varphi$ (degrees)	37	35	–	–	–	–
$v_{\rm strm}$ (km s^{-1})	2726	2060	1570	–	–	–
v_0 (km s^{-1})	307	361	–	–	–	–

[a] Bartzakos et al. (1995);
[b] Seggewiß, Moffat & Lamontagne (1991);
[c] Moffat et al. (in preparation);
[d] Moffat, Niemela & Marraco (1990).

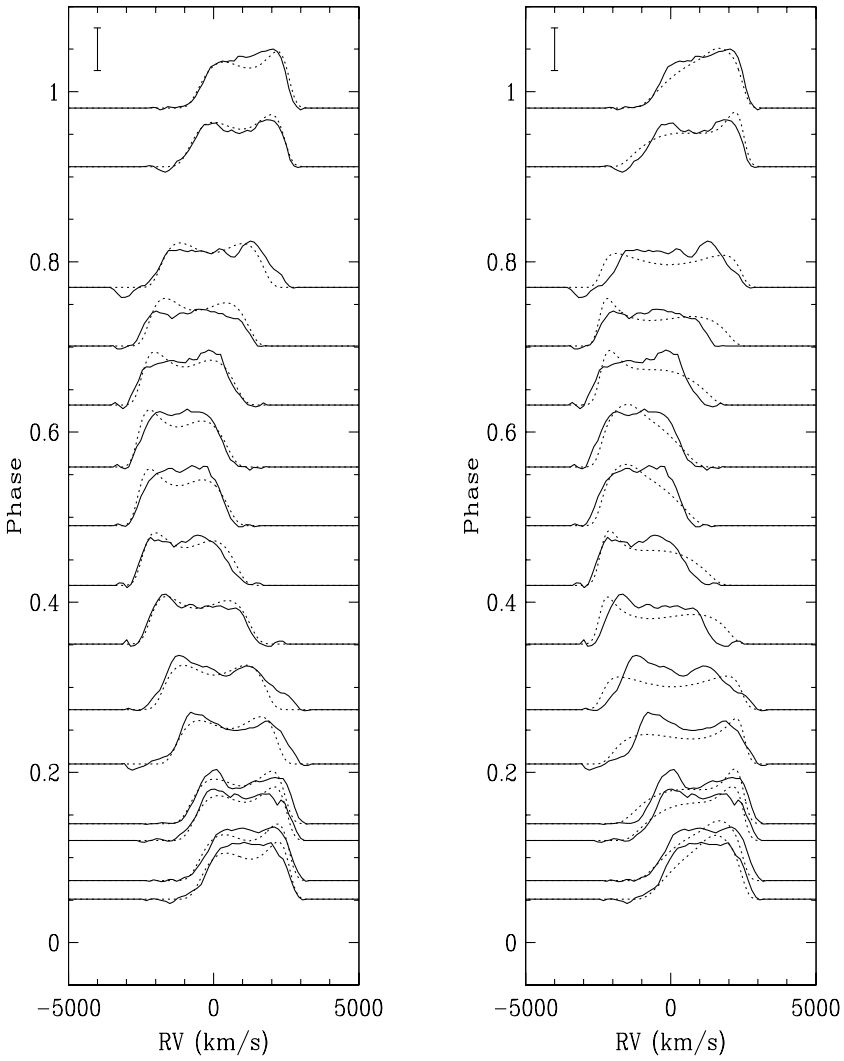

Figure 6. Lührs' model fit to the 1993 November C III 5696-Å spectra of WR 9. The left-hand plot shows the fit for inclination as a variable parameter, while the right-hand side shows the results with a fixed inclination of $i = 68°$. The solid lines represent the data, truncated to zero outside the excess profile, while the dotted lines show the corresponding instrumentally smoothed model fits. Here the wavelength is in the inertial frame of the centre of mass of the system. The vertical bar height indicates 25 per cent of the continuum intensity.

Table 2. Parameter values of the Lührs model fit to the 1993 November spectra of the CIII 5696-Å line for WR 9 (for inclination both as a variable fit and as a fixed parameter).

Parameter	Simultaneous fit	Simultaneous fit (fixed i)	Polarimetry[a]
θ_1 (degrees)	0.1	0.4	–
θ_2 (degrees)	47	90	–
i (degrees)	30	(68)	68
$\delta\varphi$ (degrees)	10	10	–
$v_{\rm strm}$ (km s^{-1})	2798	2496	–
v_0 (km s^{-1})	2	39	–

[a]Moffat et al. (in preparation).

3.3 WWC parameters from excess mean radial velocity and FWHM variations of C III 5696 Å

As an alternative to profile fitting, Lührs also measured the location, in Doppler velocity space, of the double peaks of the excess emission of C III 5696 Å for WR 79. He then fitted $v_{x_0} - v^*$ and $v_{x_0} + v^*$ to the corresponding blue and red peak positions, respectively, to obtain various parameters of the shock cone and the inclination of the binary system (Lührs 1991, 1997), where the mean excess velocity $v_{x_0} = v_{\rm strm}\cos\theta\sin i\cos 2\pi\varphi$, and the half-separation of the peaks $v^* = v_{\rm strm}\sin\theta\sqrt{1-\sin^2 i\cos^2 2\pi\varphi}$.[1] Although these values have the merit of being directly derived from the physical quantities described by these equations, locating the peak positions can be difficult. The two peaks might not even be obvious (as in many spectra of Br22). Attempting to use the method of fitting to peak positions thus becomes unreliable. Such an effort, for Br22, was made by Bartzakos, Moffat & Niemela (1995); the positions of missing peaks were roughly compensated for by choosing the location of the profile intensity just before it falls off rapidly.

[1] Note that Lührs took the origin of phases at inferior conjunction of the O star, as opposed to our definition, in this paper, at inferior conjunction of the WR star.

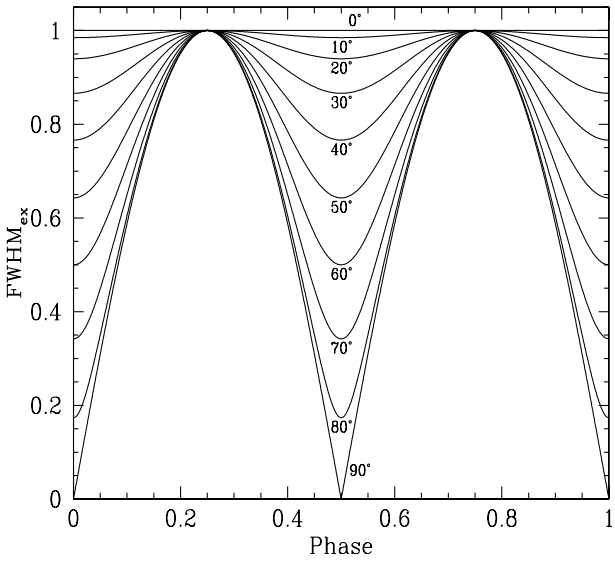

Figure 7. FWHM$_{ex}$, based on Lührs' model, as a function of orbital phase plotted for various inclinations at 10° increments. Each curve is labelled with its inclination. Here $c_1 = 0$, $c_2 = 1$ and $c_4 = 0$. See also Fig. 10 for normalized curves.

Another related alternative, which is impervious to the sometimes ambiguous location of the two peaks, is to measure and fit the mean radial velocity and the FWHM of the excess emission as a function of orbital phase. To do this, it is assumed that one can write those two quantities in the form

$$\bar{v}_{\rm ex} = \text{constant} + v_{x_0} \tag{1}$$

$$= a_1 + a_2 \cos 2\pi(\varphi - a_3) \tag{2}$$

and

$$\text{FWHM}_{\rm ex} = \text{constant} + 2v^* \tag{3}$$

$$= c_1 + c_2\sqrt{1 - c_3 \cos^2[2\pi(\varphi - c_4)]}, \tag{4}$$

in which the fitted parameters are

$$a_1 = \text{constant}, \tag{5}$$

$$a_2 = v_{\rm strm} \cos\theta \sin i, \tag{6}$$

$$a_3 = \delta\varphi, \tag{7}$$

$$c_1 = \text{constant}, \tag{8}$$

$$c_2 = 2v_{\rm strm} \sin\theta, \tag{9}$$

$$c_3 = \sin^2 i, \tag{10}$$

and

$$c_4 = \delta\varphi. \tag{11}$$

The constant a_1 represents the systemic velocity while the constant c_1 represents an approximate FWHM extension of the observed excess profile beyond either idealized peak. To illustrate the dependence of FWHM$_{ex}(\varphi)$ on i, equation (4) is plotted for various values of orbital plane inclination in Fig. 7. Although a_3 and c_4 both represent the same quantity, they were fitted separately for the sake of convenience.

It is assumed here that the separation of the two peaks and the observed FWHM differ by the same constant for all phases, which might not be precisely true in reality. For lack of a better objective technique, this was used nevertheless as a working model. This method was applied to C III 5696 Å on both Br22 and WR 9 for the 1993 November data (the best and most complete set).

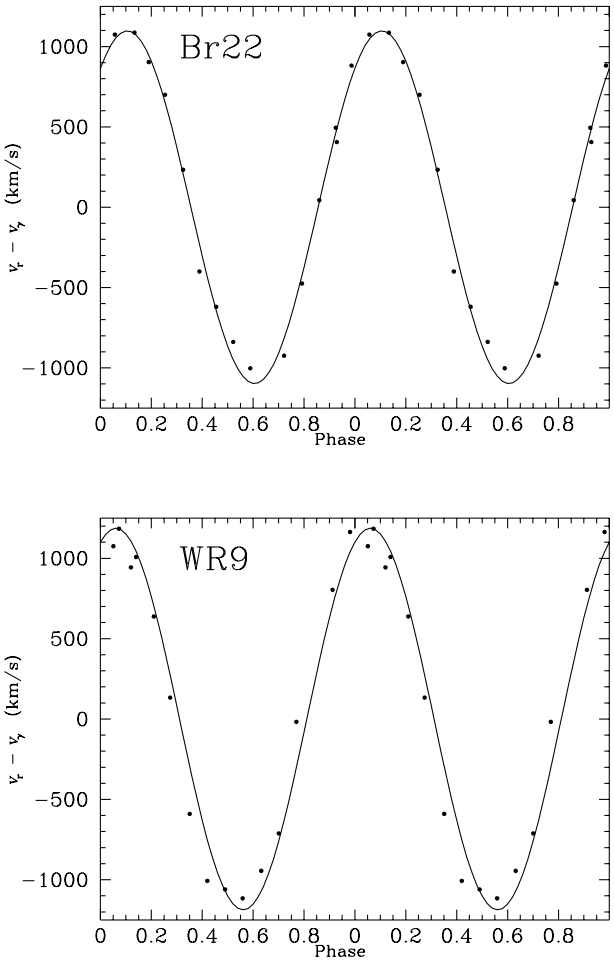

Figure 8. Fit to C III 5696-Å mean radial velocity of excess profiles of Br22 and WR 9. The same data are repeated over two orbital cycles. Phases are based on the WR-star orbit.

The mean radial velocities and FWHM of the excess emission were calculated in the same way as they were for the global C IV 5808-Å line described in Paper I. The mean radial velocities were then fitted to equation (2) in the same manner as the radial velocities were fitted to circular orbits in Appendix A, with the fixed period taken from Tables A2 and A3. The FWHM were fitted to equation (4) with the non-linear least-squares routine MRQMIN of Press et al. (1992, pp. 675–683).

The results of the radial velocity fits of the excess emision for both Br22 and WR 9 are illustrated in Fig. 8, while those for the FWHM fit are illustrated in Fig. 9. The values of the WWC parameters are listed in Table 3, as derived from equations (6), (7), (9), (10) and (11). Results for variable as well as fixed inclination are shown. It is quite clear that the fit with variable inclination yields results that are absurd. The errors on some parameters are very high (c_1 and c_2). In fact, the values of the parameters themselves are unrealistically high: for Br22, $v_{\rm strm}$ is higher than the expected terminal speed of the WR wind. In addition, there is an unphysical negative result for c_1 in Br22. The fit with fixed inclination (based on independent information) gives parameter results that have much smaller errors (see Table 3).

It appears that the fit is not very sensitive to inclination. In Fig. 10 equation (4) is plotted for various values of *i*. All curves are normalized to the same amplitude. Relatively little change occurs between solutions for different inclinations, except for values near $i = 90°$. The fit solution could, therefore, very well be numerically degenerate in *i*, given the scatter in the data.

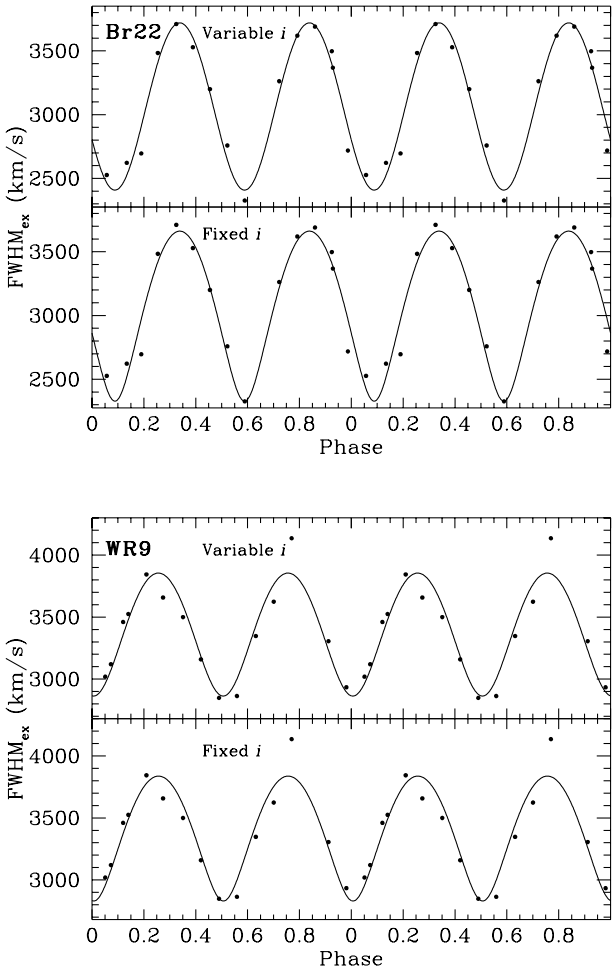

Figure 9. Fit to C III 5696-Å FWHM of excess profiles of Br22 and WR 9 (variable and fixed inclination). The same data are repeated over two orbital cycles.

3.4 Excess emission in C IV 5808 Å

Other emission lines in the binary WR stars also exhibit profile variations (cf. Fig. 1). In particular, the strong CIV 5808-Å doublet and the CIII/CIV 4650-Å complex show clear variations with orbital phase. A description of a qualitative study of the CIV 5808-Å line follows. Note that this line is a doublet (5802/5812), although the 10-Å separation of the two components is relatively small compared with the overall linewidth in all cases (FWHM > 50 Å). Worse than this is the superposition of the blue edge of He I 5876 Å on the red wing of C IV 5808 Å, on which the FWHM depends. However, He I 5876 Å is relatively weak in WC4/WO stars, and it can be neglected to first approximation. The 4650-Å emission complex (C III 4650 + C IV 4658 + He II 4686) is much more complicated and it is ignored, despite its large variations.

The excess emission profiles for C IV 5808 Å were found in the same manner as were those for C III 5696 Å. A minimum profile was defined, but, unlike the C III line, this profile was much higher and was also assumed to be round-topped, as in single WC/WO stars (Fig. 11). Again, the minimum profile was arbitrarily taken as the greatest possible emission produced by the WR wind (as was done for the C III 5696-Å line but without making C IV 5808 Å flat-topped).

This base profile was then subtracted from each spectrum of C IV 5808 Å in the WR frame and the remainder shifted back to

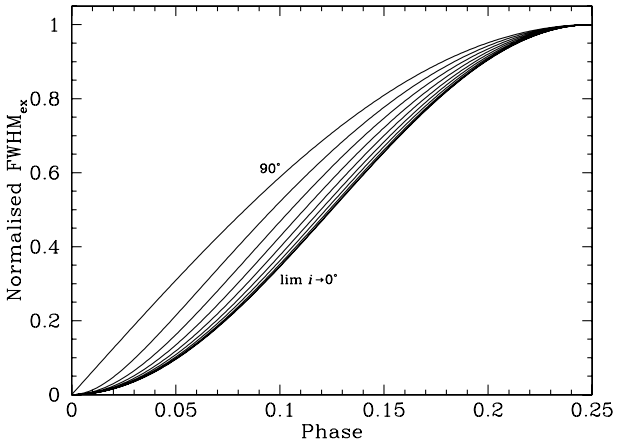

Figure 10. Normalized profiles of $FWHM_{ex}$ for 10° increments in inclination from phase $\varphi = 0°$ to 0°.25. The curves with inclinations of 90° and $\lim_{i\to 0}$ are labelled.

Table 3. Shock cone parameters derived from mean radial velocity and FWHM fits to the C III 5696-Å excess emission. Results for both variable and fixed inclination are given.

Parameter	Br22		WR 9	
a_1 (km s^{-1})	245 ± 22		-19 ± 24	
a_2 (km s^{-1})	1097 ± 32		1187 ± 32	
a_3 (degrees)	38 ± 14		22 ± 44	
	Variable *i*	Fixed $i = 71°$[a]	Variable *i*	Fixed $i = 68°$[a]
c_1 (km s^{-1})	$-2800 \pm 13\,700$	1680 ± 120	1500 ± 2600	2230 ± 120
c_2 (km s^{-1})	$6600 \pm 13\,800$	1980 ± 150	2300 ± 2700	1610 ± 16
c_3	0.36 ± 0.67	0.894 ± 0	0.666 ± 0.565	0.860 ± 0
c_4 (degrees)	32 ± 2	32 ± 2	2 ± 3	2 ± 3
i (degrees)	37 ± 40	(71)	55 ± 34	(68)
v_{strm} (km s^{-1})	3800 ± 6100	1520 ± 55	1870 ± 970	1510 ± 53
θ (degrees)	60 ± 58	40 ± 2	39 ± 37	32 ± 3

[a] Moffat et al. (in preparation).

the observer's frame of reference. The results are illustrated in Fig. 12.

The plots of the Magellanic Cloud stars in Fig. 12 reveal profiles that vary with phase. [This effect is not as clear for the Galactic stars WR 9 and WR 30a: subjected to greater interstellar extinction, they have spectra with a strong diffuse interstellar absorption feature (Herbig 1975) interfering with the emission line. This feature was manually corrected in the spectra by directly joining its extrema before obtaining the excess emission profiles shown; these net profiles appear to vary with phase nevertheless.]

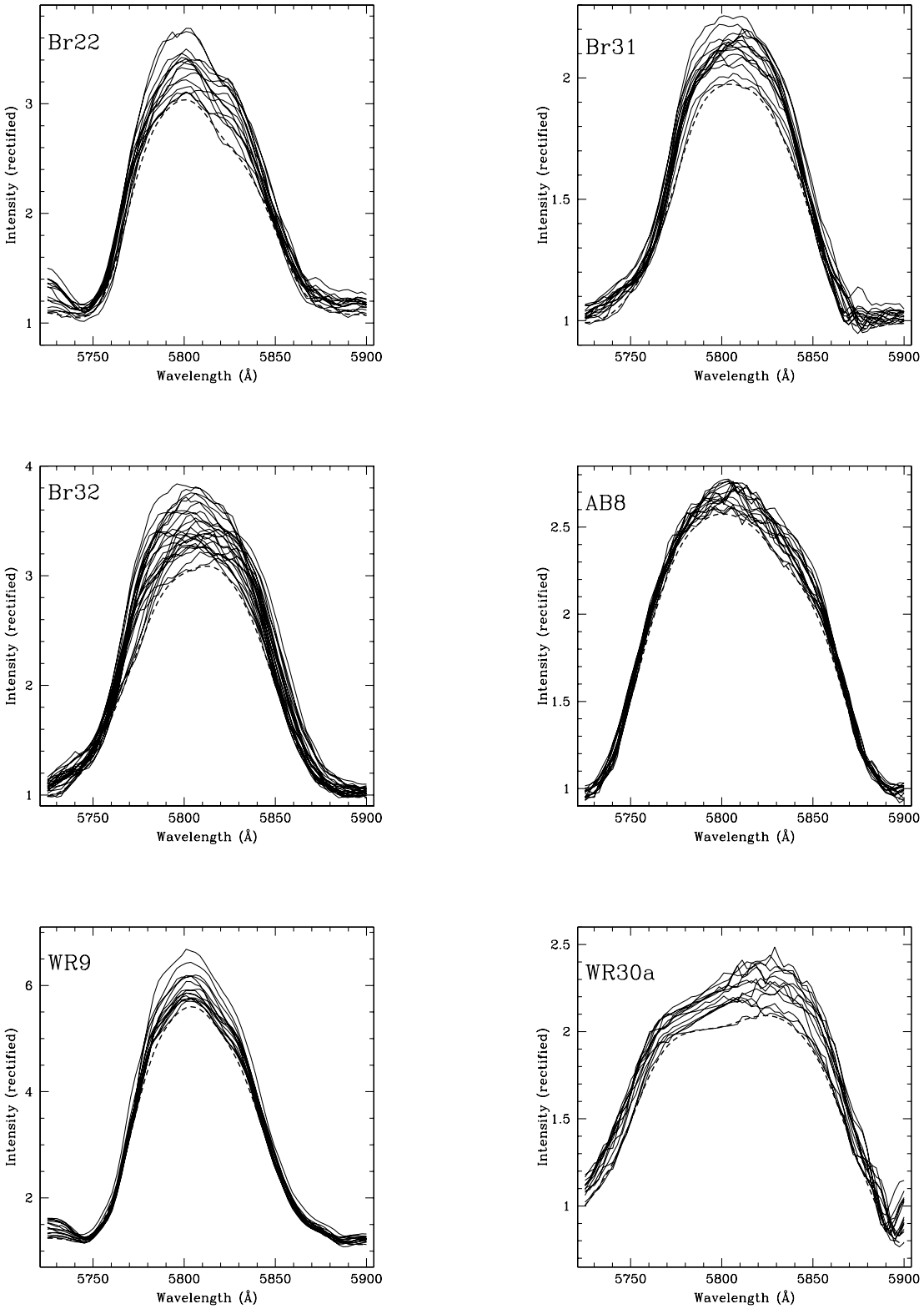

Figure 11. Superposition of spectra and assumed pedestal WR-star emission (dashed line) of C IV 5808 Å for all six binary programme stars.

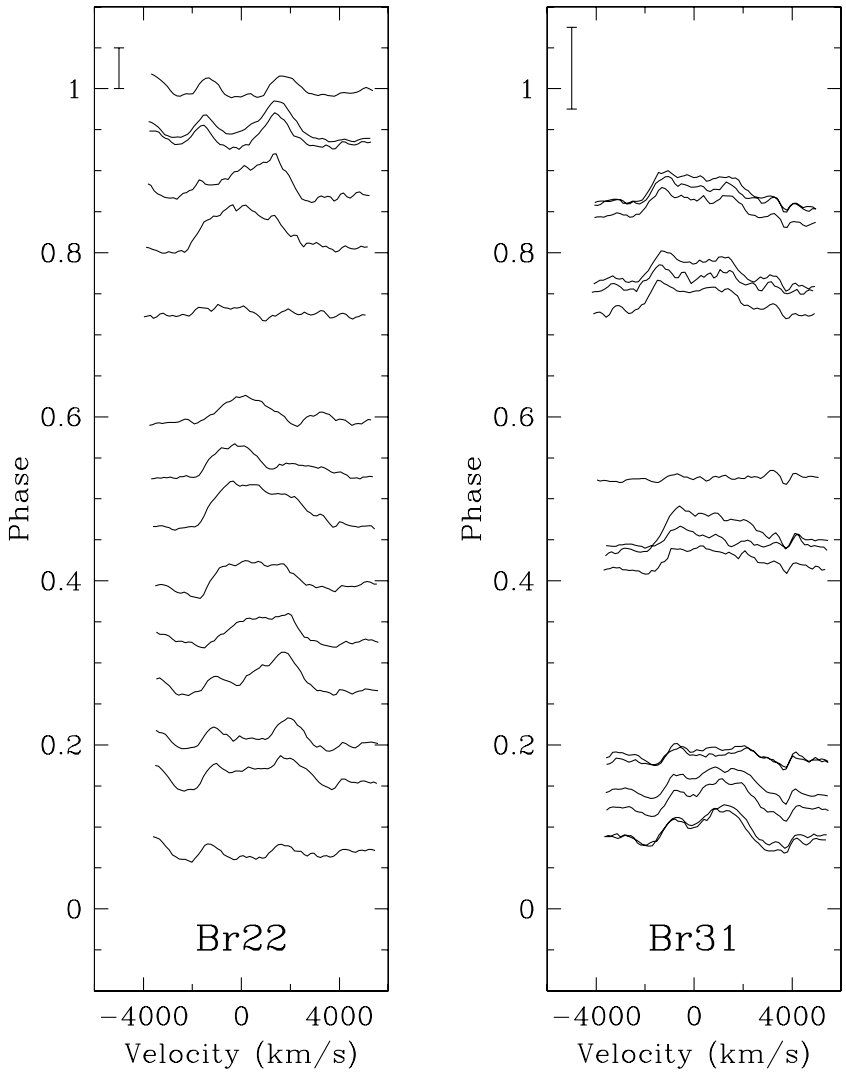

Figure 12. C IV 5808-Å excess emission profiles for the binary programme stars. The height of the error bar shows 50 per cent of the continuum intensity.

For Br32, and to a lesser extent Br31, which has large phase gaps, the net profiles tend to have single peaks near phases zero and 0.5 (when the binary is at conjunction). As the system rotates towards quadrature, the single peak spreads into two peaks that reach maximum separation near phases 0.25 and 0.75. The mean velocity of the profile does not appear to change much, however. This should be compared with the Lührs plots for a cone opening half-angle $\theta = 45°$–$135°$ (Fig. 3). Such a shock cone is akin to a rotating plane between the stars of the binary. Such an effect could be produced for a nearly planar shock cone for winds of equal momentum flux.

In the case of AB8, the peaks also merge and separate twice per orbital cycle, with the point of merging and separating appearing to be phase-shifted by about 0.06. This is probably due to a Coriolis deflection ($\delta\varphi$) of the part of the shock cone where this excess emission is produced. Also, the mean velocity of the feature varies strongly with orbital phase. This is characteristic of a cone with low to moderate opening angle (see the plots in Fig. 3 for $\theta = 10°$–$30°$ and $\theta = 22.^{\circ}5$–$67.^{\circ}5$).

The case of Br22 is similar to those of Br31 and Br32. It has two peaks that tend to separate and merge as well. Like Br32, the mean velocity of the profile varies little, indicating a large cone opening angle. The Coriolis shift is also apparent by the phase shift of the points of merging of the peaks (as in AB8). This does not necessarily contradict the results for the study of C III excess emission, where a narrower cone opening angle was extracted. The C III ions could be formed farther from the apex of the shock cone, where the flow would appear to be more nearly parallel, hence with a narrower cone angle. The more highly ionized C IV would be expected to form closer to the hotter apex, where the curvature is wider and would give the appearance of a wider cone opening angle (as the cone apex would be expected to be curved and not sharp as in the simplified Lührs model). This suggests the possibility that a study of excess emission of many different ions could permit the shock cone to be mapped out. It should be noted, however, that the subtraction process of the WR atmospheric contribution to C IV 5808 Å entails many uncertainties, making the results for the excess emission of a more qualitative nature compared with those for C III 5696 Å in Br22 and WR 9.

4 CONCLUSIONS

The WWC phenomenon is seen in all four Magellanic Cloud WC/WO binaries studied, as well as in two Galactic WC binary

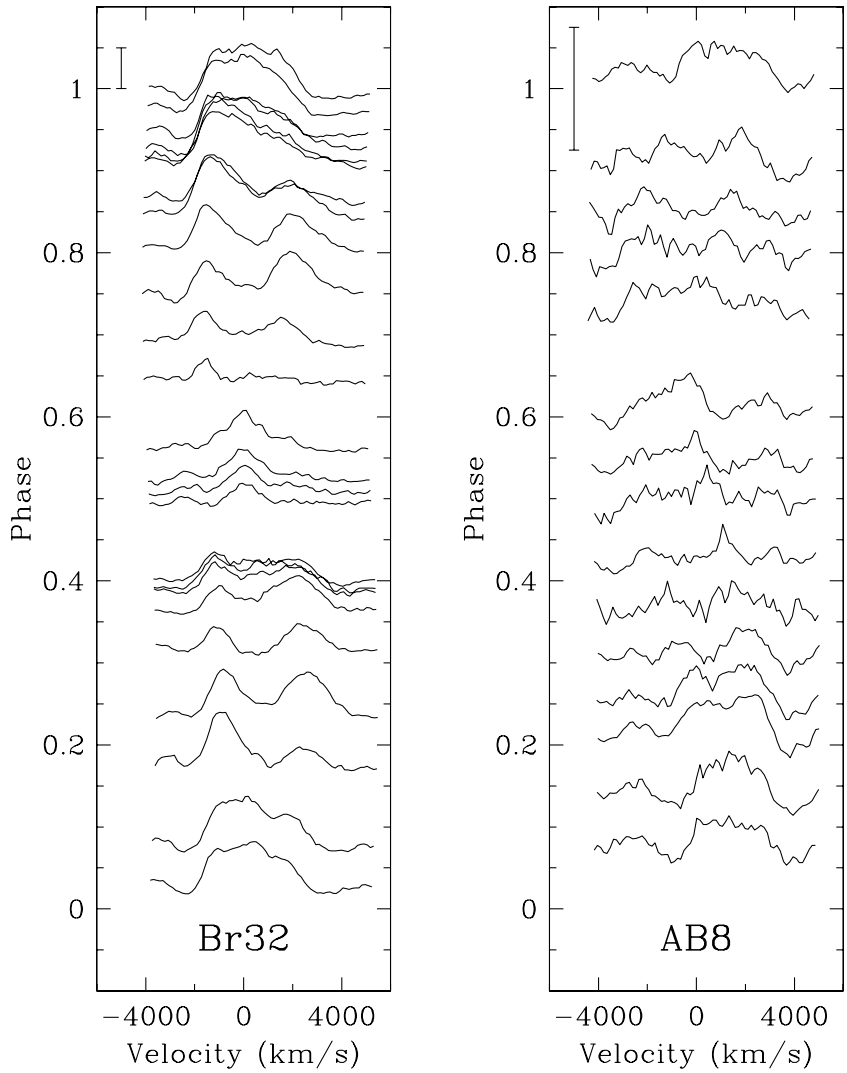

Figure 12 – *continued*

stars. Wind–wind collisions probably are a universal characteristic of binary WC/WO stars and perhaps all binary WR subtypes with short to moderate periods. As a corollary to this, the WWC excess can falsify the WR subtype, as in Br22 and WR 9 (cf. also the extreme WWC system HD 5980: Moffat et al. 1998). Allowing for this permits one to conclude that all the Magellanic Cloud WC/WO class stars are of type WC4 or WO3.

The simple Lührs model of a conical WWC shock was fitted directly to the C III 5696-Å excess emission-line data for the stars Br22 and WR 9. The model profile was able to follow the mean displacement, in velocity space, of the emission profile but was not able to mimic the detailed profile shape properly. In addition, the value obtained for an estimate of the orbital inclination was unexpectedly low and the estimated wind streaming velocity along the shock cone was unreasonably high. This might be due to the O-star cavity and/or asymmetry in the core emission, which was not allowed for. Hill et al. (2000), however, did succeed in applying the model to the Galactic WC7+O binaries WR 79 and WR 42, without having to allow for these effects.

In principle, the FWHM of the excess emission line can be used to find the inclination of the system, but the solution appears to be numerically degenerate in practice. However, if the inclination is fixed a priori, other parameters might be determined, such as the streaming velocity, the deflection of the line joining the two stars of the cone owing to Coriolis effects, and the cone opening angle, which reflects the ratio of wind momentum fluxes between the two component stars. Despite the limitations of analytic techniques such as this, they are useful to gain insight into the nature of the problem.

ACKNOWLEDGMENTS

PB is grateful to the staff of Complejo Astronómico El Leoncito for their technical assistance and hospitality during his two observing runs there. CASLEO is operated under agreement between CONICET, SeCyT and the National Universities of La Plata, Cordoba and San Juan, Argentina. PB also gratefully acknowledges financial aid provided by the Physics Department Astronomy Group of the Université de Montréal from its FCAR/équipe grant, as well as from a 'Bourse de production de mémoire et de thèse' from the FICSUM of the Fédération des associations étudiantes du campus de l'Université de Montréal. AFJM acknowledges financial support from FCAR (Québec) and the

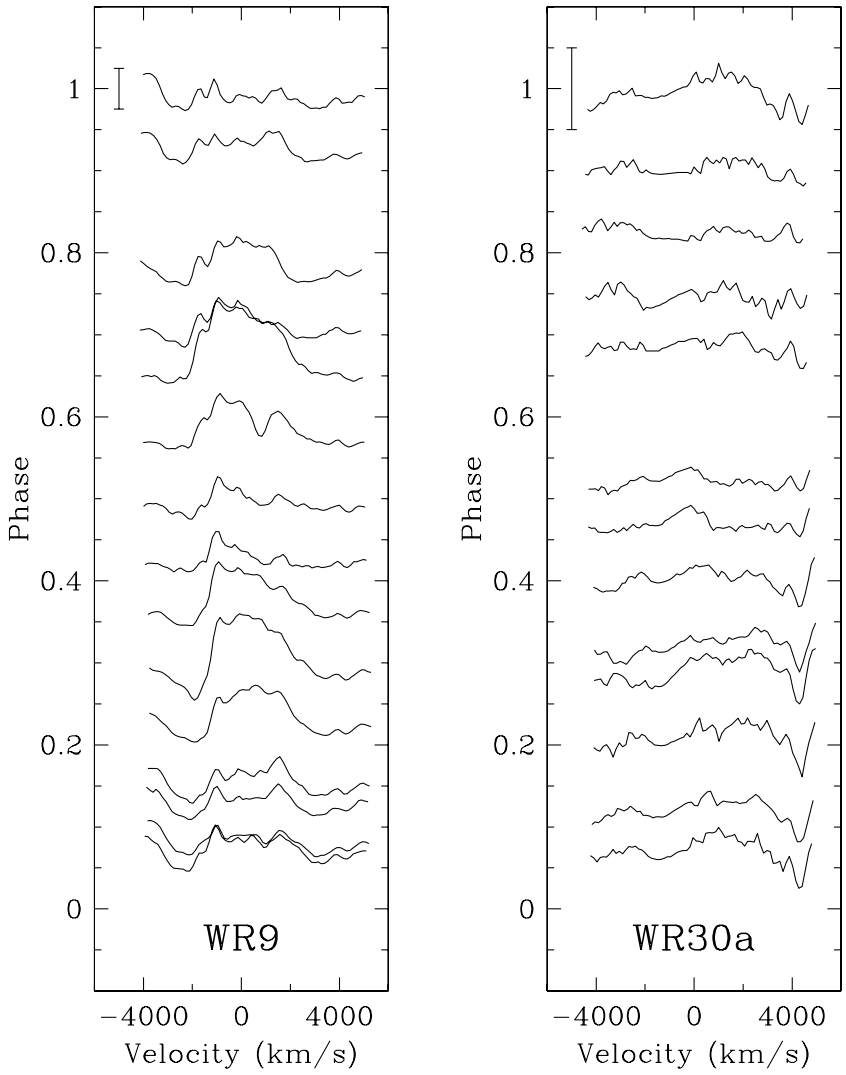

Figure 12 – *continued*

Canada Council of the Arts. AFJM and VSN are grateful to the director and staff of the Cerro Tololo Interamerican Observatory for the use of their facilities. The Cerro Tololo Interamerican Observatory (NOAO) is operated by AURA Inc. for the National Science Foundation. We acknowledge the use, at Complejo Astronómico El Leoncito, of the CCD and data acquisition system supported through US NSF grant AST-90-15827 to R. M. Rich.

REFERENCES

Bartzakos P., 1998, PhD thesis, Université de Montréal
Bartzakos P., Moffat A. F. J., Niemela V. S., 1995, in van der Hucht K. A., Williams P. M., eds, Proc. IAU Symp. 163, Wolf–Rayet Stars: Binaries, Colliding Winds, Evolution. Kluwer, Dordrecht, p. 406
Bartzakos P., Moffat A. F. J., Niemela V. S., 2001, MNRAS, 324, 18
Charbonneau P., 1995, ApJS, 101, 309
Cherepashchuk A. M., 1976, Sov. Astron. Lett., 2, 138
Cherepashchuk A. M., 1991, in van der Hucht K. A., Hidayat B., eds, Proc. IAU Symp. 143, Wolf–Rayet Stars and Interrelations with Other Massive Stars in Galaxies. Kluwer, Dordrecht, p. 187
Corcoran M. F., Stevens I. R., Pollock A. M. T., Swank J. H., Shore S. N., Rawley G. L., 1996, ApJ, 464, 434
Gayley K. G., Owocki S. P., Cranmer S. R., 1997, ApJ, 475, 786
Herbig G. H., 1975, ApJ, 196, 129
Hill G. M., Moffat A. F. J., St-Louis N., Bartzakos P., 2000, MNRAS, 318, 402
Lucy L. B., Sweeney M. A., 1971, AJ, 76, 544
Lührs S., 1991, PhD thesis, Westfälische Wilhelms-Universität Münster
Lührs S., 1997, PASP, 109, 504
Maeder A., Conti P. S., 1994, ARA&A, 32, 227
Moffat A. F. J., 1995, in van der Hucht K. A., Williams P. M., eds, Proc. IAU Symp. 163, Wolf–Rayet Stars: Binaries, Colliding Winds, Evolution. Kluwer, Dordrecht, p. 213
Moffat A. F. J., 1996, in Vreux J. M., Detal A., Fraipont-Caro D., Gosset E., Rauw G., eds, 33rd Liège Int. Astrophys. Colloq., Wolf–Rayet Stars in the Framework of Stellar Evolution. Institut d'Astrophysique, Liège, p. 199
Moffat A. F. J., Niemela V. S., Marraco H. G., 1990, ApJ, 348, 232 (MNM)
Moffat A. F. J. et al., 1998, ApJ, 497, 896
Niemela V. S., Massey P., Conti P. S., 1984, PASP, 96, 549
Petrie R. M., 1962, in Hiltner W. A., eds, Stars and Stellar Systems, Vol. II, Astronomical Techniques. Univ. Chicago, Chicago, p. 560
Press W. H., Teukolsky S. A., Vetterling W. T., Flannery B. P., 1992, Numerical Recipes in FORTRAN – The Art of Scientific Computing, 2nd edn. Cambridge Univ. Press, Cambridge
Prilutskii O. F., Usov V. V., 1976, SvA, 20, 2

Seggewiß W., Moffat A. F. J., Lamontagne R., 1991, A&AS, 89, 105
Stevens I. R., Howarth I. D., 1999, MNRAS, 302, 549
Stevens I. R., Blondin J. M., Pollock A. M. T., 1992, ApJ, 386, 265
Tassoul J.-L., Tassoul M., 1996, J. Cosmic Phys., 16, 377
Zahn J.-P., 1975, A&A, 41, 329

APPENDIX A: ORBITAL PARAMETERS

The proper study of line profile variations arising from colliding stellar winds first requires the determination of an accurate orbital ephemeris for each star so as to know the orbital phase at the time of observation. An accurate period is crucial for this. To depend on previously published periods [such as those of Moffat et al. (1990, hereafter MNM)] for AB8, Br22, Br31 and Br32 would have been unsatisfactory, since the data used in the current study span a longer interval (9 years after those of MNM). In particular, two of the stars have periods in the range of 2–3 d. The precision of the periods of MNM does not allow accurate extrapolation over the more than 1000 cycles in those short-period systems that have elapsed during the 9 years without confusing the phases unacceptably.

The two Galactic WC/WO+O binaries WR 9 and WR 30a were also studied.

A1 Period search

According to MNM, the systems Br31 and Br32 have circular orbits, while the longer period systems AB8 and Br22 have orbits of eccentricity $e \lesssim 0.2$. In view of such small values, it is fair to say that all four stars (and the two Galactic WC/WO stars WR 9 and WR 30a included in this study) have nearly circular orbits, so that the orbital period can be estimated reliably by fitting the radial velocities determined from the C IV 5808-Å emission line to a sinusoidal curve. This is the strongest and cleanest line in the spectra of each system; it is also only mildly affected by WWC, but even then also in the same cycle.

Table A1. Epoch-dependent standard deviations (km s^{-1}).

Epoch	σ_{v_e}
1984 December	33.4
1993 January	26.1
1993 November	47.2

Including the period P as a parameter to be fitted in a general elliptal orbit would have required a non-linear least-squares fit. With real, noisy data, such fits are usually unstable. Instead, the period that gave the best fit was determined independently by fitting a sinusoidal curve successively for a series of different periods (or, better, frequency, $f = 1/P$, since appropriate uniform scanning of periodicity is normally done in steps of constant f). For a given fixed frequency, f (starting at a minimum frequency, $f_{\min}$), a circular orbit was fitted to the data. The resultant χ^2 value was noted. The frequency was then augmented by a small increment, Δf, and the fit was made again, and so on.

Since the data were collected during three different runs with different instruments, three corresponding systemic velocities, $v_{84\mathrm{Dec}}$, $v_{93\mathrm{Jan}}$ and $v_{93\mathrm{Nov}}$, were also allowed for and fitted. This takes into account any velocity shifts that were not due to changes in the velocity of the binary stars (such as inevitable systematic errors in instrumental calibration, or any long-period variations arising from a possible third component). Instead of v_γ, the vector $\boldsymbol{v}_\gamma = (v_{84\mathrm{Dec}}, v_{93\mathrm{Jan}}, v_{93\mathrm{Nov}})$ was used. The model to fit then becomes

$$v_{\mathrm{r}}(t) = \boldsymbol{e}(t) \cdot \boldsymbol{v}_\gamma + K_1 \cos\left(\frac{2\pi}{P}t\right) + K_2 \sin\left(\frac{2\pi}{P}t\right), \qquad \text{(A1)}$$

where

$$\boldsymbol{e}(t) = \begin{cases} (1,0,0): & t \in 1984\ \text{December epoch} \\ (0,1,0): & t \in 1993\ \text{January epoch} \\ (0,0,1): & t \in 1993\ \text{November epoch}, \end{cases}$$

and the radial velocity amplitude of the orbit $K = \sqrt{K_1^2 + K_2^2}$. The time of observation is t. The time of origin when the WR star passes in front is then

Table A2. Fit parameters of C IV 5808 Å for circular and elliptical orbits for the four binary Magellanic Cloud stars. All velocities are in km s^{-1} and dates are Heliocentric Julian dates (HJD) minus 244 0000. E_0 is the HJD of origin for the orbital phase, corresponding to the time of inferior conjunction of the WR component.

Parameter	Br22	Br31	Br32	AB8
P (d)	14.926 ± 0.006	3.0328 ± 0.0001	1.9169 ± 0.0001	16.633 ± 0.009
Circular orbit				
v_γ (84 Dec.)	638 ± 11	453 ± 11	442 ± 13	66 ± 10
v_γ (93 Jan.)	670 ± 12	532 ± 08	468 ± 09	50 ± 12
v_γ (93 Nov.)	617 ± 12	474 ± 12	430 ± 09	74 ± 12
K	211 ± 10	322 ± 09	291 ± 08	156 ± 10
E_0	6027.1 ± 0.1	6037.80 ± 0.01	6039.820 ± 0.009	6032.9 ± 0.1
χ^2_ν	0.49	0.89	1.64	0.50
Elliptical orbit				
v_γ (84 Dec.)	638 ± 08	451 ± 16	451 ± 26	66 ± 10
v_γ (93 Jan.)	666 ± 09	532 ± 07	455 ± 03	50 ± 13
v_γ (93 Nov.)	614 ± 09	474 ± 12	435 ± 10	74 ± 13
K	223 ± 09	325 ± 14	296 ± 18	157 ± 12
T	9022.7 ± 0.6	9017.5 ± 0.5	9038.41 ± 0.15	9322.8 ± 6.6
E_0	6056.8 ± 0.8	6043.874 ± 0.020	6042.88 ± 0.19	6057.88 ± 0.15
ω (degrees)	160 ± 15	83 ± 60	2 ± 28	197 ± 141
e	0.12 ± 0.03	0.04 ± 0.04	0.13 ± 0.05	0.03 ± 0.06
χ^2_ν	0.26	0.89	1.26	0.53
p (per cent)	0.018	34	0.38	78

Table A3. Fit parameters of C IV 5808 Å (emission) and He II 5412 Å (absorption) for circular orbits for the Galactic binaries WR 9 and WR 30a. All velocities are in km s^{-1} and dates are HJD minus 244 0000. E_0 is the HJD of origin for the orbital phase, corresponding to the time of inferior conjunction.

Parameter	WR 9		WR 30a	
P (d)	14.305[a]		4.625 ± 0.006	
Circular orbit	Emission	Absorption	Emission	Absorption
v_γ (84 Dec.)	–	–	–	–
v_γ (93 Jan.)	–	–	−90 ± 14	−22 ± 55
v_γ (93 Nov.)	321 ± 12	−7 ± 19	−68 ± 13	3 ± 30
K	186 ± 19	56 ± 28	207 ± 13	102 ± 37
E_0	6032.95 ± 0.20	6039.2 ± 1.1	6038.696 ± 0.051	6036.15 ± 0.28
χ^2_ν[b]	0.65	–	1.01	–

[a] Period from Niemela, Massey & Conti (1984), since they based it on more observations and over several epochs. They give no error and it is assumed here to be 0.001. The period found with the data described in the present study is 15.6 ± 3.2 d, based on only one epoch.
[b] For the absorption, no error estimates are available to yield χ^2_ν.

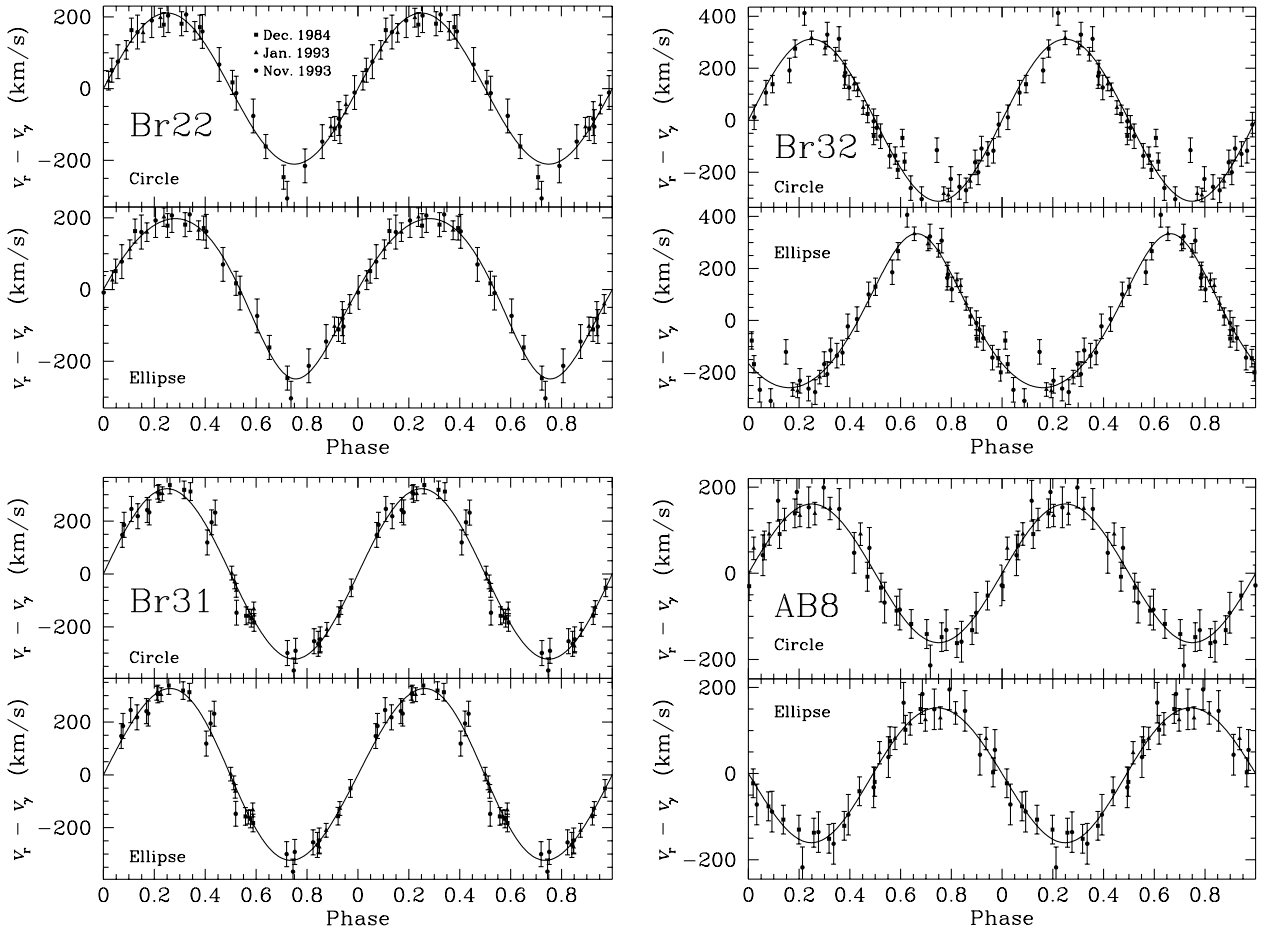

Figure A1. Circular and elliptical radial fits to C IV 5808 Å of the four certain Magellanic Cloud binaries. The velocities shown are the observed radial velocities with the epoch-dependent systemic velocities subtracted. A different point shape is used for each epoch of observation. The origins of the phases are based on E_0 for circular orbits and T for elliptical orbits.

$$t_0 = -\frac{P}{2\pi}\arctan\frac{K_1}{K_2}.$$

The routine used for the general, linear least-squares fit of the model described in equation (A1) was SVDFIT of Press et al. (1992, pp. 665–675). The standard errors of the data used in the χ^2 minimization process were chosen based on the rms dispersion in the radial velocities of the single WC stars (of Paper I). Different standard errors (σ_{v_e}) were so determined for each run (Table A1).

The radial velocities used to make the period fit in C IV 5808 Å (and the orbital fits later) are listed on the CDS web site (http://cdsweb.u-strasbg.fr/).

The results of the fitting procedure were examined to determine which frequency gave the best circular orbit fit. This frequency, however, was not necessarily the frequency ultimately chosen to yield the period closest to the true period. Unpublished period searches, undertaken by MNM as part of their study of the same four Magellanic Cloud WC/WO binary stars, were based mostly on other older data. The period ultimately chosen was that which corresponded to a local minimum χ^2 in both cases combined, even if it was not necessarily the period of absolute minimum χ^2 in either case.

The periods of the six WC/WO binary stars are listed in Tables A2 and A3. The error in the period for the Magellanic Cloud systems was estimated by finding the extent of the interval about the best period within which the change in the reduced χ^2 would be no greater than unity. The circular fits are plotted in Fig. A1.

A2 Radial velocity orbital parameters

As a test for non-zero eccentricity, an elliptical orbit was also fitted to the radial velocity data of each star. The equation of such a curve is

$$v_r(t) = v_\gamma + K[\cos(\nu + \omega) + e\cos\omega], \tag{A2}$$

where ω is the angle between the ascending line of nodes of the system and the direction of periastron, ν is the true anomaly (the angle in the orbital plane from periastron to the position of the star, as seen from the centre of mass), and e is the eccentricity of the orbit. The quantities $v_r(t)$, v_γ and K are defined previously. A derivation of this radial velocity curve is given by Petrie (1962). [Note that the excess emission from WWC will distort the line profiles, even in C IV 5808 Å (see Section 3.4). This is not allowed for here, since the effect is relatively small for C IV 5808 Å. In addition, the orbits based on this line are in anti-phase with the undistorted O-star photospheric absorption lines (MNM).]

As for the sine-wave fits, v_γ is replaced by the systemic velocity for each epoch so that equation (A2) is transformed to

$$v_r(t) = \boldsymbol{e}(t)\cdot\boldsymbol{v}_\gamma + K[\cos(\nu + \omega) + e\cos\omega]; \tag{A3}$$

$\boldsymbol{e}(t)$ and $\boldsymbol{v}_\gamma$ are as in equation (A1).

The true anomaly is related to time via

$$\tan\frac{\nu}{2} = \sqrt{\frac{1+e}{1-e}}\tan\frac{E}{2},$$

with the eccentric anomaly, E, found from

$$E - e\sin E = \frac{2\pi}{P}(t - T) \equiv M,$$

where M is the mean anomaly. T is the time of periastron passage.

The C IV 5808-Å radial velocity data were fitted by equation (A3) using E04UPF, a non-linear least-squares optimizing routine from the NAG FORTRAN library. The parameters fittted were $\boldsymbol{v}_\gamma$, K, ω, T and e (P, taken from the period found from circular fits, was fixed). Errors on these parameters were estimated from the diagonal of the covariance matrix, itself derived from the Jacobian matrix that was calculated at the optimal point (Press et al. 1992, pp. 666–667, 676–678).

The results for both circular and elliptical fits for the Magellanic Cloud binaries are listed in Table A2 and are displayed in Fig. A1. Only circular fits for the two Galactic stars are listed in Table A3, with curves shown in Fig. A2. Both emission-line curves and He II 5412-Å absorption-line orbits were studied

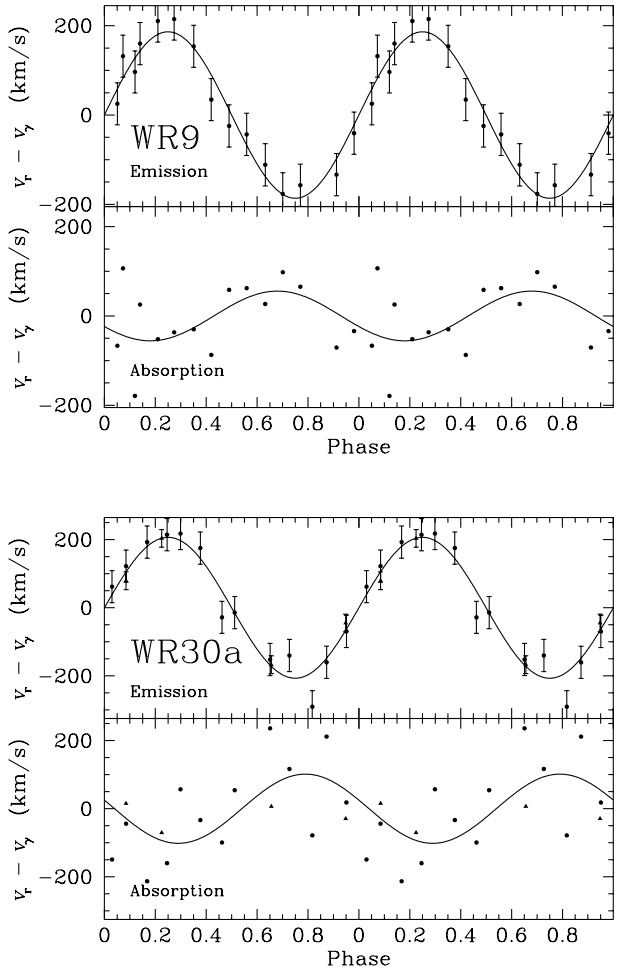

Figure A2. Circular radial velocity fits of absorption and emission features of the two Galactic WC stars. Phase refers to the emission orbit. The symbols are the same as in Fig. A1.

for the Galactic stars (the absorption-line velocities were estimated by applying Gaussian fits to the line profiles, with a sloping base estimated from neighbouring points of the He II emission line of the WR star).

Included in Table A2 is a measure of the probability that the eccentricity found could have exceeded that found for a random set of data from a circular orbit (p). This is calculated using the statistical test of Lucy & Sweeney (1971), derived from the theory of testing multivariate linear hypotheses. In two Magellanic Cloud cases, the elliptical model fits the data better then does the circular model. However, it cannot be assumed that the orbits are *necessarily* eccentric. These fits might be *mathematically* better simply because there are additional parameters that can be adjusted to generate curves that reduce the value of χ^2. The model, however, might be *physically* less plausible than its circular counterpart.

In the cases of Br31 and AB8, the ratio χ^2_ν of the circular fit to that of the eccentric orbital fit is very close to unity (1.00 and 0.94, respectively). Their p-values are well above the 5 per cent significance level. In addition, the error in the eccentricities for the elliptical models of both stars is comparable to the fit eccentricities themselves, making them indistinguishable from zero. (MNM claimed, however, an eccentric orbit for AB8 based on fewer, noisier data.)

The elliptical fit for the star Br22 yields an eccentricity that is far greater than its formal error. In addition, the ratio of circular fit to elliptical fit χ^2_ν values is considerably greater than unity (1.85). It also has a very small value for p. Br22 might have an elliptical orbit (but see later).

For Br32, MNM asumed a circular orbit because of its very short period. However, its fit eccentricity in the present data set is significantly larger than its error. Its ratio of circular-to-elliptical fit χ^2_ν is 1.28, greater than the equivalent ratios for Br31 and AB8 but substantially less than that for Br22. It also has a low value for p, suggesting that the eccentricity might not be spurious.

Should it be assumed that Br32 has a physically real elliptical orbit on the basis of this mathematical result? A brief theoretical discussion on binary rotation might be enlightening.

A system has the least mechanical energy when it rotates uniformly. The motions of stars in binaries that do not have circular orbits have stresses and strains that dissipate the mechanical energy as heat. Such stars eventually reach a state of minimum mechanical energy with circular orbits (and synchronized spins) (Tassoul & Tassoul 1996).

Stars of short period (and, therefore, closer together) will have greater straining and energy loss rate than those of longer period. Zahn (1975) calculated that, for binary massive stars of short period (such as Br32), the circularization and synchronization time ($\sim 10^5$ yr) is much less than the nuclear lifetime of approximately 10^7 yr. As the evolved component in Br32 is of WR class, it is near the end of its nuclear burning time and its orbit is expected to have become circularized long ago. Br32 is presumed, therefore, to have a circular orbit, and it is assumed that the mathematically superior model with non-zero eccentricity is probably not physically real.

To study further the possibility of eccentricity in the orbit of Br22, a radial velocity fit was made using the velocities determined from the He II 5412-Å absorption line. In this fit, the period and the eccentricity were fixed to the corresponding values shown in Table A2. The resulting fit had a very high error on ω (129°). Although these data are noisy, this suggests that there must be little or no eccentricity and that the result from fitting the velocity of the emission profiles may merely be mathematical, without physical meaning. Br22 is thus considered to have a circular orbit. All known Magellanic Cloud WC/WO binary stars, therefore, probably have circular orbits. In any case, Roche lobe overflow, if present, should have helped to circularize these orbits.

Ultimately, the shapes of the orbits would be best determined using the photospheric absorption lines, mainly in the blue, of the companion O stars. Being formed at the surface of the star and free of WWC distortions, they are more likely to reflect true orbital motion than are WR emission lines. However, since the best of these photospheric absorption lines were observed during only one epoch, the orbits of the O companions of the Magellanic Cloud binaries were not studied further. They were better determined by MNM. Nevertheless, such an attempt was made for the Galactic WC/WO binaries with the He II 5412-Å absorption feature only. The results are listed in Table A3, with the fit models displayed in Fig. A2. The times of zero phase for emission and absorption differ by 6.2 ± 1.1 d [$(0.43 \pm 0.08)P$] for WR 9 and 2.5 ± 0.3 d [$(0.54 \pm 0.06)P$] for WR 30a. Within the errors, these differences are compatible with half an orbital cycle, as expected if they reflect truly orbital motion. The mass ratio for WR 9 is $M_{\rm WR}/M_{\rm O} = 0.30 \pm 0.15$ and that for WR 30a is 0.50 ± 0.18. These are in the range found for other WC binaries in general (Cherepashchuk 1991).

Neglecting Br31 and Br32, for which the O-companion radial velocities may be reduced by the dilution effect of visual unseparated companions (see Paper I), the mass ratios $M_{\rm WR}/M_{\rm O}$ are in the range 0.3–0.4, within the errors, for the four remaining systems. Assuming initial ratios greater than one, these small values are expected for highly evolved WR stars reaching the WC4/WO stage via extreme mass loss (e.g. Moffat 1995).

This paper has been typeset from a TEX/LATEX file prepared by the author.